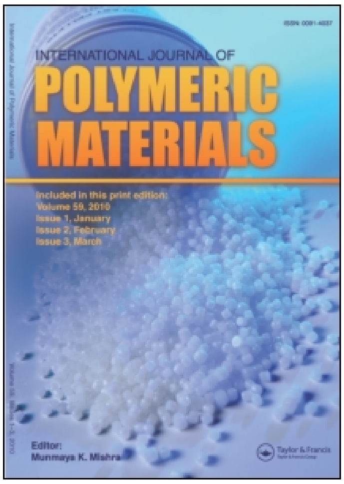

International Journal of Polymeric Materials
Publication details, including instructions for authors and subscription information:
http://www.informaworld.com/smpp/title~content=t713647664

Modeling and Simulation of a Cellulose-Acetate Blend Ultrafiltration Membrane using Bovine Serum Albumin Solution

M. Subas Chandra Bose[a]; G. Arthanareeswaran[b]; M. Raajenthiren[a]
[a] Department of Chemical Engineering, Anna University, Chennai, India [b] Department of Chemical Engineering, National Institute of Technology, Tiruchirappalli, India

To cite this Article Bose, M. Subas Chandra , Arthanareeswaran, G. and Raajenthiren, M.(2010) 'Modeling and Simulation of a Cellulose-Acetate Blend Ultrafiltration Membrane using Bovine Serum Albumin Solution', International Journal of Polymeric Materials, 59: 8, 588 — 606

To link to this Article: DOI: 10.1080/00914031003760717

URL: http://dx.doi.org/10.1080/00914031003760717

International Journal of Polymeric Materials, 59:588–606, 2010
Copyright © Taylor & Francis Group, LLC
ISSN: 0091-4037 print/1563-535X online
DOI: 10.1080/00914031003760717

Modeling and Simulation of a Cellulose-Acetate Blend Ultrafiltration Membrane using Bovine Serum Albumin Solution

M. Subas Chandra Bose,[1] G. Arthanareeswaran,[2] and M. Raajenthiren[1]

[1]Department of Chemical Engineering, Anna University, Chennai, India
[2]Department of Chemical Engineering, National Institute of Technology, Tiruchirappalli, India

In the present work, a numerical simulation of an ultrafiltration (UF) process of BSA solution through flat sheet membranes is carried out by solving the convective diffusion Eq. (CDE) for mass balance to predict permeate flux behavior in a dead end UF cell. Using the trust-region nonlinear regression technique, the experimental data obtained for flux and observed rejection of CA/SPEEK blend membranes were curve fitted to obtain the values for the permeability coefficient (P_m), reflection coefficient (σ) and mass transfer coefficient (k). The model is tested for numerical stability and accuracy by varying key numerical parameters such as the numerical time step (Δt).

Keywords numerical simulation, permeate flux, polymer membrane, Spiegler-Kedem model, ultrafiltration

INTRODUCTION

Ultrafiltration is a process where the high molecular weight component, such as a protein molecule, and suspended solids are rejected, while all low molecular weight components, such as NaCl, pass through the membrane freely.

Received 17 December 2009; in final form 7 March 2010.

Address correspondence to G. Arthanareeswaran, Department of Chemical Engineering, National Institute of Technology, Tiruchirappalli-620015, India. E-mail: arthanaree10@yahoo.com; arthanareeg@nitt.edu

Membrane separation processes such as reverse osmosis and ultrafiltration have gained considerable importance because they offer superior treatment at relatively modest capital and operating costs. The processes remove a wide range of contaminants present in untreated water and municipal and industrial wastewater discharges such as suspended and dissolved solids, organic matter, heavy metals, bacteria and viruses.

Theoretical concentration polarization studies are centered around obtaining solutions for mass transport and flow balance (Navier-Stokes Eqs.). Approximate solutions are only available for systems where several simplifying assumptions are made; these include constant fluid and solute properties, simplified fluid flow profiles and steady-state analysis. The last assumption is a major limitation to the predictive capability of a model. In most membrane systems, concentration polarization reaches steady state within a few hours of operation but permeate flux continues to decline over time because of fouling and membrane degradation. In order to address this problem correctly, a predictive transient model for concentration polarization is necessary that will allow for dynamic phenomena to be included at a latter stage. The initial transient data generated from such a model could be used to understand the conditions that develop and exist near the membrane surface. Such information could be used in improving the physical aspects of the model, and correct mechanistic assumptions that are made in developing the model.

Another limitation of existing work is that commercial systems are rarely taken into account. In real systems, there are several complicating factors such as feed stream characteristics, membrane type (UF, RO), module type (plate and frame, hollow-fiber, spiral wound), and ambient conditions. The flow profiles in commercial modules are usually distorted and complex because of mixing and turbulence from feed spacers. These effects are very important especially in full-scale systems that operate at moderate to high recoveries (permeate flow per unit feed flow), and should be included to improve overall design.

Once the system has been characterized, a simulation model has been suggested for the prediction of flux and rejection that involves performing calculations as a function of time. Thin-film theory is used to describe the membrane surface boundary conditions, and the osmotic pressure model is used to describe the membrane permeation behavior. The model resulting from film theory visualization of the mass transfer process is then used in generating permeate flux decline behavior for several feed and membrane characteristics. The data is obtained from MATLAB code for the simulation model resulting from the convective diffusion equation. The combined Spiegler-Kedem/film theory model (CFSK) is used for parameter estimation using a trust-region algorithm in MATLAB [1]. Experimental data for parameter estimation was obtained from a batch-type, continuous stirred, dead-end UF cell using CA/SPEEK blend membranes.

EXPERIMENTAL

Materials and Methods

CA/SPEEK blend ultrafiltration membranes in the composition of 100/0, 90/05, 85/15, 75/25 and 65/35 wt% were prepared and characterized [2]. Bovine serum albumin (BSA), a protein with MWCO of 69 kDa, was purchased from SRL Chemicals Ltd., India, and used as received. Disodium hydrogen orthophosphate anhydrous and monosodium dihydrogen orthophosphate heptahydrate were procured from CDH Chemicals Ltd., India. The MATLAB software package was purchased from Mathworks, Inc., and used for the simulation and modeling of CA/SPEEK blend membranes.

Characterization of Membranes

The ultrafiltration experiments were carried out in a 400 ml batch-type stirred cell (ultrafiltration cell—S76-400-Model, Spectrum, USA) fitted with a Teflon-coated magnetic paddle (as shown in Figure 1). The effective membrane area available for ultrafiltration was 38.5 cm^2. The solution filled in the cell was stirred at 400 rpm using a magnetic stirrer. All the experiments were carried out at 30 ± 2°C. The different blend composition of CA/SPEEK membranes are shown in Table 1. All the blend membranes were characterized for their ultrafiltration performance.

Membrane Resistance

Membrane resistance (R_m), which denotes the intrinsic resistance of the membrane, was measured with pure water as the feed [3]. Hydraulic

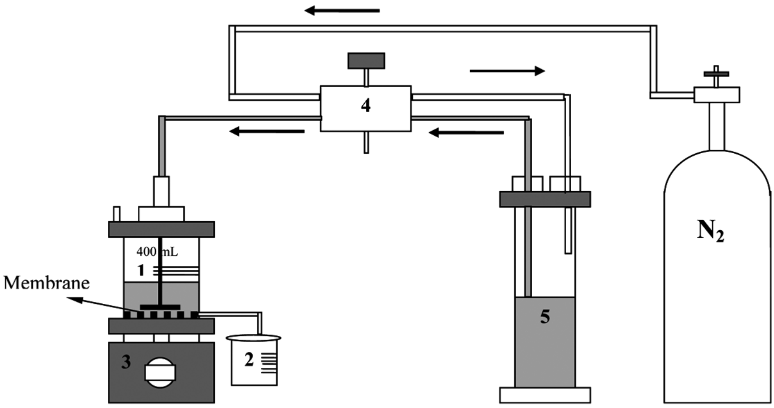

(1) stirred UF cell (2) permeate (3) magnetic stirrer (4) selector (5) pressure reservoir

Figure 1: Experimental set up of ultrafiltration process.

Table 1: Permeate flux of BSA by CA/SPEEK blend membranes.

Blend composition[a] (wt%)		Permeate flux
CA %	SPEEK %	$(J_v) \times 10^{-3}\,m^3/m^2h$
100	0	14.6
95	5	15.7
85	15	32.4
75	25	56.7
65	35	65.4

resistance of clean membrane, R_m, is an indication of tolerance of the membrane towards hydraulic pressure. After the pure water flux reached steady state, R_m is determined by measuring the pure water flux under various transmembrane pressures from 69 to 414 kPa. R_m was calculated from the inverse of slope of the corresponding pressure vs. pure water flux plot (Figure 2) using the following Eq.(3) [4].

$$J_w = \left(\frac{\Delta P}{R_m}\right) \tag{3}$$

where, J_w is pure water flux in m^3/m^2h, ΔP is transmembrane pressure in kPa. R_m is membrane resistance in $kPa \cdot h/m$. The membrane resistance for different blend compositions is tabulated in Table 2.

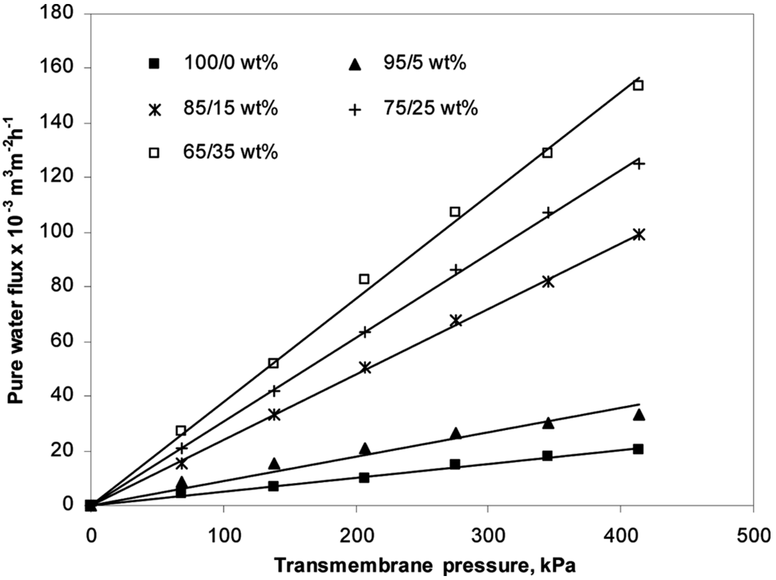

Figure 2: Effect of transmembrane pressure on pure water flux of CA/SPEEK blend membranes.

Table 2: Membrane hydraulic resistance, R_m, of CA/SPEEK blend membranes.

Blend composition[a] (wt%)		
CA %	**SPEEK %**	**$R_m \times 10^3$ (kPa · h/m)**
100	0	19.9
95	5	9.2
85	15	4.2
75	25	3.2
65	35	2.6

Molecular Weight Cut-Off (MWCO) and Average Pore Size

Molecular weight cut-off is an attribute of pore size of the membranes and is related to the rejection of a spherical solute of given molecular weight. The molecular weight has a linear relationship with the pore size of the membrane [5]. In general, the molecular weight cut-off of the membrane is determined by identifying an inert solute of the lowest molecular weight that has a solute rejection of 80–100% in steady state UF experiments [6]. Thus, the proteins of different molecular weights such as BSA (69 kDa), pepsin (35 kDa) and trypsin (20 kDa) were taken for rejection studies of the membranes. Aqueous solutions of bovine serum albumin (BSA), pepsin and trypsin were prepared at a concentration of 1000 mg/l by dissolving the proteins (0.1 wt%) individually in a phosphate buffer (0.5 M, pH 7.2). The UF cell was filled with protein solution and pressurized at a constant pressure of 345 kPa and stirred throughout the experiments to minimize fouling. During ultrafiltration, the permeate solutions of corresponding membranes were collected over a period of time in a graduated tube and were analyzed for the concentration of protein by UV-visible spectrophotometer (Shimadzu, Model UV-160A) at 280 nm. From the feed and permeate concentrations, the percentage rejection was calculated using the equation reported in previous literatures [5,7].

The average pore size and surface porosity were determined by the ultrafiltration of protein solutions of different molecular weights. From protein removal studies as described below, the molecular weight of the solute (protein) that has a solute rejection (%SR) above 80% was used to evaluate the average pore size, $\overline{R}$, of the membranes by the following [7,8].

$$\overline{R} = 100\left(\frac{\alpha}{\%SR_0}\right) \tag{4}$$

where $\overline{R}$ is the average pore size (radius) of the membrane (Å), and α is the average solute radius (Å). The average solute radii, also known as the Stoke radii, were obtained from the plot of solute molecular weight vs. solute radius

Table 3: Average pore radius and MWCO of CA/SPEEK blend membranes.

Polymer composition (wt%)[a]		Average pore radius R (Å)	MWCO (kDa)
CA %	SPEEK %		
100	0	11.5 (0.22)	20
95	5	12.3 (0.13)	35
85	15	15.2 (0.15)	35
75	25	19.5 (0.13)	69
65	35	25.3 (0.21)	69

Note: Numbers in the parenthesis are standard deviation.

in an aqueous solution, which was developed by Sarbolouki [8]. The MWCO and average pore size of the membranes determined from the protein rejection studies are shown in Table 3.

EXPERIMENTAL STUDIES ON CONCENTRATION POLARIZATION

Rejection and Permeate Flux Studies

Flat asymmetric, hydrophilic CA/SPEEK blended membrane was used to predict the permeate flux and observed rejection of BSA protein solution. Bovine serum albumin was dissolved (0.1 wt %) in a phosphate buffer (0.5 m, pH 7.2) and used as a standard solution. After the characterization, the membranes were mounted in the ultrafiltration cell, the feed reservoir was filled with the protein solution and pressurized under nitrogen atmosphere at 345 kPa and maintained constant throughout the run. The pH of the feed solution was kept constant at 7.2 since the change in pH may increase the adsorptive fouling of the membranes [4]. The permeate from the cell was collected over measured time intervals in graduated tubes, and the permeate flux was calculated by using [9].

$$J = \frac{Q}{A \cdot \Delta T} \tag{1}$$

where, J = Permeate flux,m^3/m^2h; Q = quantity of permeate, m^3, A = membrane area, m^2; ΔT = sampling time, h. The tube contents were analyzed to determine the protein concentration by spectrophotometry at λ_{max} of 280 nm using a Hitachi U-2000 spectrophotometer. The percentage of observed rejection of BSA solution was evaluated from the concentration of the feed and permeate using [2].

$$\%\, SR_o = \left[1 - \frac{C_p}{C_f}\right] \times 100 \tag{2}$$

Table 4: Observed rejection of BSA by CA/SPEEK blend membranes.

Blend composition[a] (wt%)		
CA %	**SPEEK %**	**Observed rejection of BSA (R_0)**
100	0	0.92
95	5	0.91
85	15	0.87
75	25	0.81
65	35	0.77

[a] Total polymer concentration = 17.5 wt%.

where, C_p and C_f are concentrations of permeate and feed, respectively. The flux and observed rejection data are tabulated in Tables 1 and 4, respectively.

ESTIMATION OF PARAMETERS

It is now recognized that a three-parameter model such as the combined Spiegler-Kedem/film theory model is much better to describe the transport processes occurring inside membranes. Hence the model is used for parameter estimation. The following section explains the theory behind the Spiegler-Kedem and film theory model.

Theory

The film model is widely in use and is a good starting point when investigating the phenomena occurring in the concentration boundary layer [10,11].

Film Theory

According to film theory the convective and diffusive transport through the film equals the solute transport through the membrane giving the mass balance

$$J_v C + D\frac{dC}{dx} = J_v C_p \tag{4}$$

Figure 3 shows the concentration profile near the membrane surface at steady state conditions. where,

J_v is the volume flux,

C_p is the concentration in the permeate and

D is the diffusion coefficient

The boundary conditions are

$$x = 0 \text{ at } C = C_m \tag{5}$$

$$x = \delta \text{ at } C = C_b \tag{6}$$

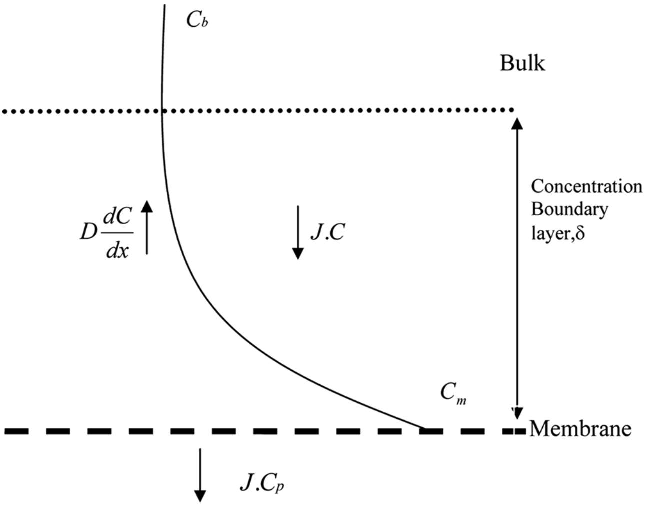

Figure 3: Mass transfer in the concentration boundary layer and through the membrane.

where, δ is the concentration boundary layer thickness. Equation (4) can be rearranged and integrated to give

$$\ln\left[\frac{C_m - C_p}{C_b - C_p}\right] = \frac{J_v\delta}{D} \tag{7}$$

or

$$\frac{C_m - C_p}{C_b - C_p} = \exp\left(\frac{J_v\delta}{D}\right) = \exp\left(\frac{J_v}{k}\right) \tag{8}$$

where $D/\delta = k$ is the mass transfer coefficient.

Introducing the definition for the intrinsic retention coefficient Eq. (9),

$$R_r = \frac{C_m - C_p}{C_m} = 1 - \frac{C_p}{C_m} \tag{9}$$

and rearranging, Eq. (7) can be written as

$$\frac{C_m}{C_b} = \frac{\exp\left(\frac{J_v}{k}\right)}{R_r + (1 - R_r)\exp\left(\frac{J_v}{k}\right)} \tag{10}$$

This is called the concentration polarization modulus. Equation (8) can be presented in a linearized form [10].

$$\ln\left(\frac{1 - R_o}{R_o}\right) = \ln\left(\frac{1 - R_r}{R_r}\right) + \frac{J_v}{k} \tag{11}$$

Combined Spiegler-Kedem/Film Theory Model

This three-parameter model [12,13] based on the concept of irreversible thermodynamics starts with a differential equation for fluxes, given by

$$J_A = P_s\left(\frac{dC}{dx}\right) + (1-\sigma)CJ_v \tag{12}$$

Putting, $J_A = C_p J_v$

$$P_s = \left(\frac{dC}{dx}\right) + [(1-\sigma)C - C_p]J_v = 0 \tag{13}$$

Integrating Eq. (13) with boundary limit as

$$x = 0, C = C_p \tag{14}$$

and

$$x = \Delta x, C = C_m \tag{15}$$

$$\int_{C_p}^{C_m} \frac{dC}{(1-\sigma)C - C_p} + \int_0^{\Delta x} \frac{J_v dx}{P_s} = 0 \tag{16}$$

This on integration gives

$$\frac{C_p - C_m(1-\sigma)}{\sigma C_p} = \exp\left[-\frac{J_v(1-\sigma)}{P_m}\right] \tag{17}$$

where, $P_m = P_s/\Delta x$. Making R_r the subject of Eq.

$$\frac{1}{1-R_r} = \frac{1}{1-\sigma} - \frac{\sigma}{1-\sigma}\exp\left[-\frac{J_v(1-\sigma)}{P_m}\right] \tag{18}$$

Substituting Eq. (11) in Eq. (18) to eliminate R_r will result in the following form:

$$\frac{R_o}{1-R_o} = \frac{\sigma}{1-\sigma}\left[1 - \exp\left\{\frac{J_v(1-\sigma)}{P_m}\right\}\right]\exp\left(-\frac{J_v}{k}\right) \tag{19}$$

In the above equation, the unknown parameters are as follows:

$$A = \frac{\sigma}{1-\sigma}, B = \frac{1-\sigma}{P_m}, C = \frac{1}{k} \tag{20}$$

In this study experimental data for permeate flux, J_v and observed rejection, R_o were obtained from experiments. These data (Tables 1 and 4) were curve-fitted using a MATLAB curve-fitting toolbox, which is part of the MATLAB software package, from Mathworks, Inc. MATLAB is a high-performance language for technical computing with many built-in functions for solving differential equations. This curve-fitting toolbox uses the nonlinear

Table 5: Parameter values obtained from the nonlinear parameter estimation method using trust-region algorithm in MATLAB curve fitting toolbox.

Membrane Permeability, P_m	9.51×10^{-3} m/s
Reflection coefficient, σ	0.8463
Mass transfer coefficient, k	8.11×10^{-6} m/s

least squares formulation to fit a nonlinear model to data. The algorithm that was used to obtain the values of the parameters A, B and C was "Trust region". It can solve difficult nonlinear problems more efficiently than the other algorithms and it represents an improvement over the popular Levenberg-Marquardt algorithm [14,15]. The two variables involved in this model are $(R_o/1-R_o)$ and J_v which are correlated by a nonlinear equation as given. Eq. (19) [12] was curve-fitted using the experimental data to obtain the values of the parameters A, B and C [16] P_m, σ and k were calculated using Eq. (20) [17]. The parameter values obtained (Table 5), were used to simulate flux and rejection under particular operating conditions for the fixed solute membrane concentration.

RESULTS AND DISCUSSION

Simulation of Membrane Performance

During the past few decades, various experimental techniques have been developed for the monitoring of concentration polarization in order to better understand the physicochemical processes governing the development of a polarized layer of solutes near a membrane surface. Such techniques enable the testing of theoretical models and, more importantly, provide valuable information on the mechanisms governing the development of concentration polarization in membrane filtration. To simulate permeate volumetric flux and permeate concentration based on the membrane parameters P_m, σ and k determined by using the procedure explained above, a transient solution of convective-diffusion equation was done coupled with an osmotic pressure model (Eq. (26)).

Assumptions and Basic Features of the Model

1. The feed solution consists of one solute (bovine serum albumin), component 1, and a solvent (water).
2. The model assumes that the membrane is permeable to solute (Rejection R is less than or equal to 1).
3. The boundary conditions are defined as in the case of stirred-batch ultrafiltration, using the thin-film model. Isothermal conditions exist.

4. Finally to simplify computing complexity in the initial start-up period, it is assumed that fluid flow is fully developed and at a steady state at the start of each run.

5. Constant density and diffusivity.

Simulation

The nonconservative form of the mass balance convective diffusion equation was used to generate concentration polarization (CP) information and permeate flux behavior. The equation is written as [18]

$$\frac{\partial C}{\partial t} = J_v \frac{\partial C}{\partial z} + D \frac{\partial^2 C}{\partial z^2} \tag{21}$$

where, C is the concentration of the solute on the feed side in kg/m^3 and is a function of spatial coordinate z in m and time t, J_v is fluid velocity in m/s, and D is the solute diffusivity in m/s. The mass balance convective-diffusion equation is a second-order partial differential equation that requires two initial conditions, one boundary condition in the axial direction.

The appropriate initial and boundary conditions are

$$\text{At t} = 0, \mathrm{C_A} = \mathrm{C_b} \text{ for all z} \tag{22}$$

$$\text{At z} = 0, \mathrm{C_A} = \mathrm{C_m} \text{ for t} > 0 \tag{23}$$

$$\text{At z} = \delta, \mathrm{C_A} = \mathrm{C_b} \text{ for t} > 0 \tag{24}$$

The parabolic partial differential equation can be written in the following form using the forward time central space finite difference scheme as [9,19]

$$\begin{aligned} C(i+l,j) = C(i,j) + \Delta t \Bigg[& D \frac{C(i,j-1) - 2C(i,j) + C(i,j+1)}{\Delta x^2} \\ & + J_v \frac{C(i,j-1) - C(i,j+1)}{2\Delta x} \Bigg] \end{aligned} \tag{25}$$

The volumetric flux can be determined by using the osmotic pressure model given by the following: [20]

$$J_v = \frac{\Delta P - \sigma \Delta \pi}{\mu_s R_m} \tag{26}$$

where, $\Delta\pi = \pi_m - \pi_p = \pi(C_m) - \pi(C_p)$.

The osmotic pressure of a solution can be determined experimentally by using a membrane osmometer. The results from such studies were fitted by using the following polynomial: [21]

$$\pi = 204.78C - 2.0C^2 + 8.44 \times 10^{-3} C^3 \tag{27}$$

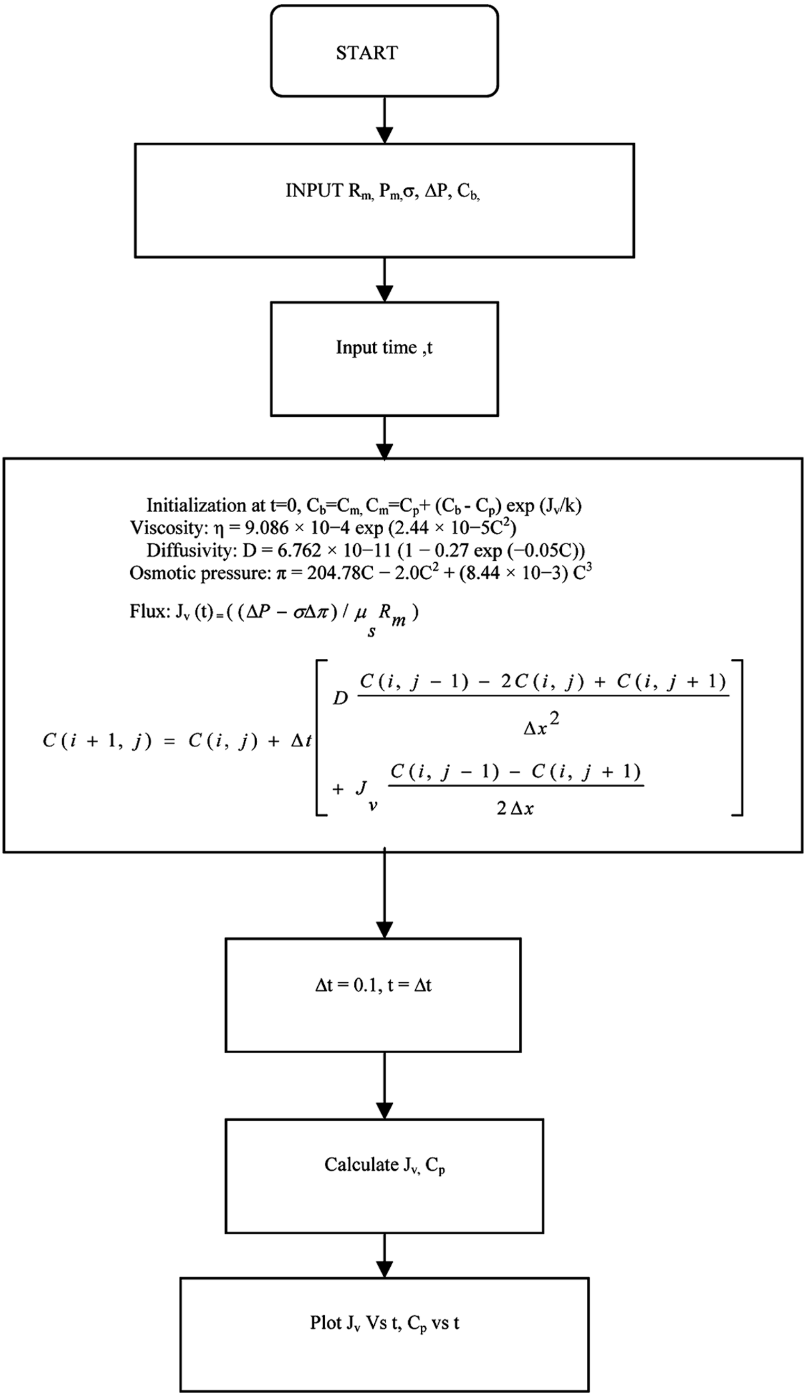

Figure 4: Algorithm for simulation of membrane performance.

Apart from the above correlation the following correlations were also used in the simulation algorithm. The viscosity and diffusivity were correlated to the concentration of BSA at 30°C as follows: [22,23]

$$\eta = 9.086 \times 10^{-4} \exp(2.44 \times 10^{-5} C^2) \tag{28}$$

$$D = 6.762 \times 10^{-11}(1 - 0.027 \exp(-0.05C)) \tag{29}$$

Algorithm

The simulation is based on an iterative scheme; the simulation algorithm is given in Figure 4. During the simulation BSA permeate flux and rejection of 100/0, 95/05, 85/15, 75/25 and 65/35 wt% blend composition of membranes, and the values of reflection coefficient (σ), solute permeability (P_m), and mass transfer coefficient (k) were used in the computation along with all membrane hydraulic resistance determined from the experiment. The values for σ, P_m, k resulting from the nonlinear parameter estimation method are 0.8463 and 9.51×10^{-3} m/s, 8.11×10^{-6} m/s, respectively. The average membrane hydraulic resistance, R_m, was found to be 7.82×10^{3} kPa · h/m. The proposed simulation approach is a three-parameter model, requiring the values of R_m, σ and P_m. Once the above three parameter values are known, calculations can be started to obtain the volumetric flux and permeate concentration as a function of time, starting from $t = 0$ to any desired time. The initialization step, as mentioned in the proposed algorithm, was found to provide convergence in all the circumstances. Further, the time increment (Δt) is an important user-defined parameter which has to be fixed a priori. Δt was assumed to be 0.1 s, which was found to give reasonable accuracy.

MATLAB code was written [24] for carrying out the simulation procedure mentioned in Figure 4. The convective-diffusion equation which is a partial differential equation was replaced with a suitable algebraic difference quotient, a finite difference for generating the data of permeate flux decline behavior for several feed and membrane characteristics, and the following simulation results are obtained.

EXPERIMENTAL STUDIES ON CONCENTRATION POLARIZATION

Rejection and Permeate Flux Studies

It is generally accepted that concentration polarization of solute at the membrane surface can lead to solute adsorption, solute precipitation and gel layer formation. In the case of UF membranes, this all results in a decrease in the permeate water flux across the membrane. This, in turn, increases operating costs due to the need for frequent membrane cleaning and possibly

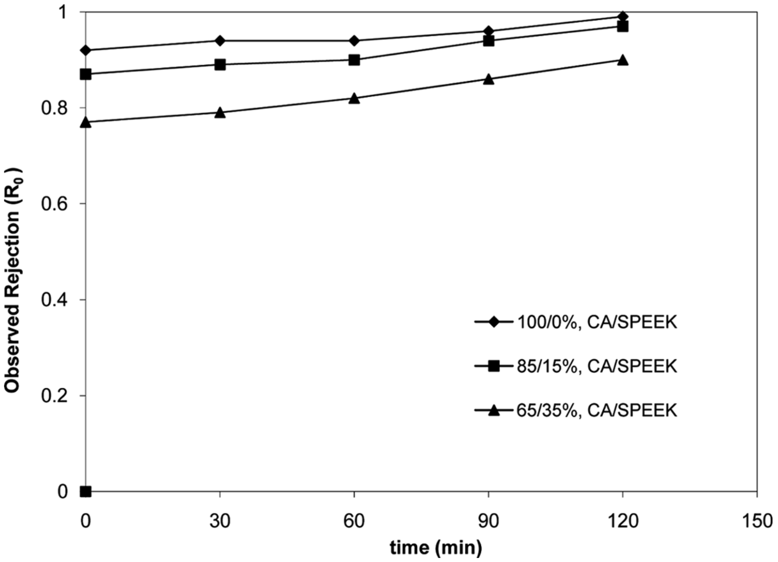

Figure 5: Experimental measurement of observed rejection of BSA as a function of bulk concentration vs. time for 100/0, 85/15 and 65/35 wt% blend CA/SPEEK membranes (at 345 kPa TMP, $C_b = 30\,kg/m^3$).

reduced membrane lifetime. In this study, the experimental work on concentration polarization in UF membranes was focused on measurement of permeate flux and solute rejection of BSA solution.

The effect of filtration time on $\%R_0$ and permeate flux of BSA solution, for 100/0, 85/15 and 65/35 wt% of CA/SPEEK blend membranes at a constant pressure of 345 kPa, are shown in Figures 5 and 6, respectively. The increase in filtration time results in a significant decrease in BSA observed rejection (R_0). This may be due to the increasing concentration polarization with time on the membrane. Also, when the SPEEK concentration is increased from 0 to 65 wt% in the CA polymer, a corresponding decrease in BSA observed rejection from 0.92 to 0.77 at initial filtration time as depicted in Figure 5. Further, at 120 min filtration time, the observed rejection values of 100/0 to 65/35 blend composition of CA/SPEEK blend membranes were decreased from 0.99 to 0.90.

From Figure 6, it is seen that there is always a substantial decline in the permeate flux with time, due to the development of a polarized layer of solutes near a membrane surface. They also indicated that flow decline depends on the pore and molecule size distributions of the prepared membranes. In addition, they showed that a declined permeate flux contributed to a lower membrane resistance. From Figure 6, the permeate flux of 65/35 wt% blend membrane was $65.4\,m^2/m^3s$, which is higher then other blend compositions. Further, the permeate flux value of of 65/35 wt% blend

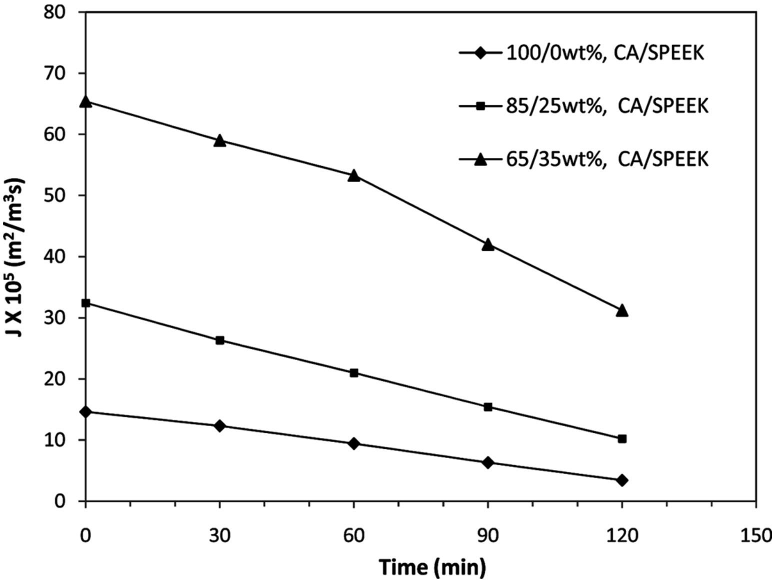

Figure 6: Experimental measurement of permeate flux of BSA as a function of bulk concentration vs. time for 100/0, 85/15 and 65/35 wt% blend CA/SPEEK membranes (at 345 kPa TMP, $C_b = 30\,kg/m^3$).

membrane ($31.2\,m^2/m^3s$) was decresed at 120 min. Thus, based on our discussion, the decrease of permeate flux with time may be due to the development of a disordered solute layer above the membrane surface.

Figure 7 shows the theoretical predictions of BSA permeate flux as a function of bulk concentration with time. The theoretical predictions were based on film theory and the combined Spiegler-Kedem/film theory model with a pressure governed permeate flux. Three different sets of bulk concentrations 10, 20, and $30\,kg/m^3$, respectively were used under constant pressure of 345 kPa and the program was run to obtain flux as a function of bulk concentration with time, since the model used is a transient model. The obtained results proved the fact that an increase in bulk concentration means more solute deposition on the membrane surface, which offers additional resistance to separation at the membrane surface. Therefore the higher the membrane surface concentration, the larger the effect of concentration polarization. These will cause the flux to decline with increasing bulk concentration. Flux was found to be higher for the lower bulk concentration $10\,kg/m^3$ as compared to the higher bulk concentration $30\,kg/m^3$. The permeate flux is modeled using membrane coefficient, flux and rejection of BSA for CA/SPEEK blend membranes (100/0, 95/05, 85/15, 75/25 and 65/35 wt%) to predict the membrane permeability, reflection coefficient, mass transfer coefficient. The models found the decline of BSA permeate flux at different concentrations of all blend membranes. In case of experiments, the permeate flux was measured at $30\,kg/cm^3$ BSA

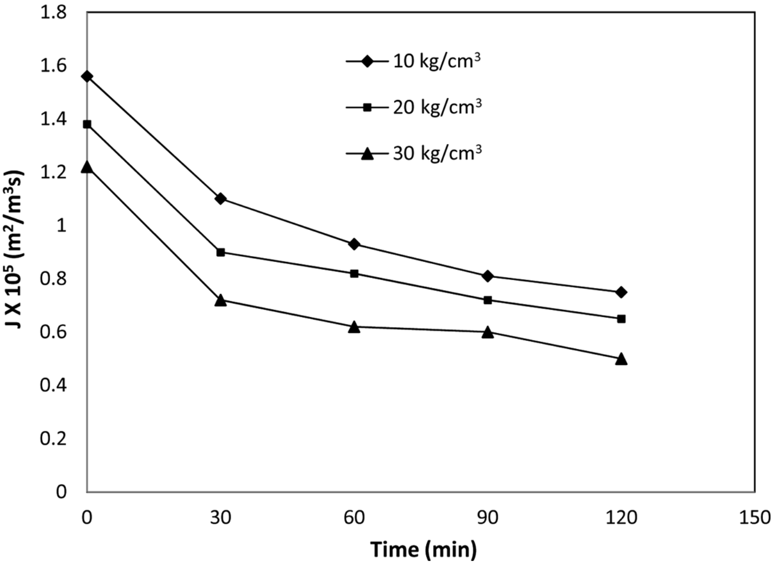

Figure 7: Variation of simulated permeate flux of BSA as a function of bulk concentration vs. time for all blend compositions of CA/SPEEK blend membranes (at 345 kPa TMP, $C_b = 10$, 20, 30 kg/m^3, respectively).

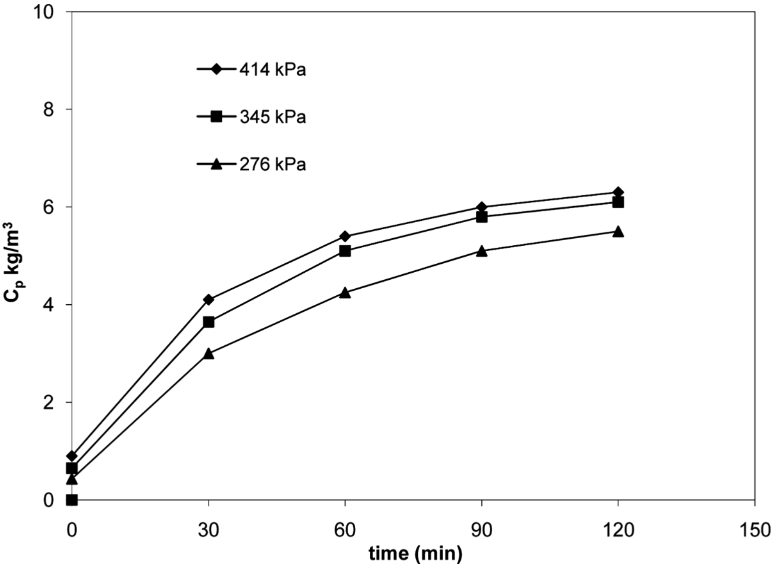

Figure 8: Simulated permeate concentration of BSA as a function of pressure vs. time for all blend compositions of CA/SPEEK blend membranes ($C_b = 10$ kg/m^3, TMP at 276, 345, 414 kPa, respectively).

concentration for 100/0, 85/35 and 65/35 wt% of CA/SPEEK blend membranes. Hence, reasonable adjustment of the permeate flux resulted in the same trend between theoretical prediction and experimental results. Carme et al. [25] observed the same trend for the separation of protein mixtures.

Figure 8 shows the permeate concentration as a function of pressure with time for the following transmembrane pressures of UF 276, 345, and 414 kPa, respectively, and constant bulk concentration 10 kg/m^3. The permeate concentration was estimated simultaneously from the simulation algorithm. The obtained permeate concentration for transmembrane pressure 414 kPa was found to be higher than those found for lower pressures 345 and 276 kPa. During the simulation under constant bulk concentration, the permeate concentration of BSA for the entire blend of CA/SPEEK membranes was increased with increasing time. This is because with an increase in pressure, the flux increases, causing more driving force through the membrane, as a result more solute permeates through the membrane and hence the permeate concentration increases. A similar trend was observed by Bhattacharjee et al. [26] for asymmetric cellulose acetate membrane.

CONCLUSION

The work investigates concentration polarization and resulting permeate flux decline in flat sheet polymeric CA/SPEEK ultrafiltration membranes. Concentration polarization is a serious problem that decreases permeate throughput and quality, increases operating costs and results in frequent membrane cleaning and replacement. The proposed simulation model is a transient model that can be used to obtain permeate flux behavior and permeate concentration (hence rejection) as a function of time under specified transmembrane pressure and bulk concentration. The predicted results from the model comply with the assumptions made in the model and general concepts regarding separation of protein solutes by ultrafiltration. Simulation results were obtained by using solute permeability, reflection coefficient and mass transfer coefficient values, calculated by CFSK model. Results showed the same trend of permeate flux with time, between experiments and model predictions. The effects of change in the bulk concentration and TMP on the parameters estimated from the Trust region nonlinear regression technique have been established.

NOMENCLATURE

C	concentration of the macro-ion (BSA) [kg/m^3]
C_A	solute concentration [kg/m^3]

C_b	feed concentration [kg/m^3]
C_m	membrane surface concentration [kg/m^3]
C_p	permeate concentration [kg/m^3]
D	diffusivity [m^2/s]
J_A	solute flux through membrane [kg/m$^2 \cdot$ h]
J_v	volumetric flux [m^3/m^{2}h]
J_w	pure water flux [m^3/m$^2 \cdot$ h]
k	mass transfer coefficient [m/s]
P_m	local solute permeability per unit membrane thickness [m/s] (Permeability coefficient)
ΔP	transmembrane pressure difference [Pa]
$\Delta\pi$	osmotic pressure difference [Pa]
R_o	observed rejection, $(1 - C_p/C_b)$, (dimensionless)
R_r	real rejection, $(1 - C_p/C_m)$, (dimensionless)
R_m	resistance of membrane [kPa $\cdot$ h/m]
t	time [s]
x	distance coordinates within the membrane with origin lying on the permeate side membrane surface [m]
Δx	membrane thickness [m]
z	difference away from the membrane surface on feed side[m]

Greek Letters

δ	concentration boundary layer thickness[m]
σ	reflection coefficient, 0 for no rejection, 1 for total rejection
π	osmotic pressure [Pa]
μ_s	solution viscosity [kg/ms]
μ	viscosity [kg/ms]
Δ	difference [-]

Subscripts

b	bulk
i	component
m	membrane surface
p	permeate phase
j	component

REFERENCES

[1] Stanislaw, K. *Desalination* **198**, 335 (2006).

[2] Arthanareeswaran, G., Srinivasan, K., Mahendran, R., Mohan, D., Rajendran, M., and Mohan, V. *Euro. Poly. J.* **40**, 751 (2004).

[3] Cheryan, M. (1986). *Ultrafiltration Handbook; Technical Publishing Company*, Lancaster, U.K.

[4] Brinck, J., Jonsson, A. F., Jonsson, B., and Lindau, J. *J. Membr. Sci.* **164**, 187 (2000).

[5] Mahendran, R., Malaisamy, R., and Mohan, D. *Polym. Adv. Technol.* **51**, 149 (2004).

[6] Malaisamy, R., Mahendran, R., and Mohan, D. *J. Appl. Polym. Sci.* **84**, 430 (2002).

[7] Malaisamy, R., Mohan, D., and Rajendran, M. *J. Colloi. Interfa. Sci.* **254**, 129 (2002).

[8] Sarbolouki, M. N. *Sep. Sci. Technol.* **17**, 381 (1982).

[9] Anderson, J. D. (1995). *Computational Fluid Dynamics: The Basics with Applications*, McGraw-Hill, Inc., New York.

[10] Jonsson, G., and Boesen, C. E. (1984). *Synthetic Membrane Processes*, Academic Press, Inc., Orlando.

[11] Mulder, M. (1996). *Basic Principles of Membrane Technology*, 2nd Ed., Kluwer Academic Publishers, Dordrecht.

[12] Spiegler, K. S., and Kedem, O. *Desalination* **1**, 311 (1966).

[13] Soltanieh, M., and Gill, W. *Chem. Eng. Commun.* **12**, 279 (1981).

[14] Finlayson, B. A. (1980). *Nonlinear Analysis in Chemical Engineering*, McGraw Hill, New York.

[15] Madsen, K., Nielsen, H. B., and Tingleff, O. (2004). *Methods For Non-Linear Least Squares Problems*, 2nd Ed., Informatics and Mathematical Modeling, Technical University of Denmark.

[16] Senthilmurugan, S., Aruj, A., and Sharad, K. G. *Desalination* **173**, 269 (2005).

[17] Soltanieh, M., and Gill, W. *Chem. Eng. Commun.* **12**, 279 (1981).

[18] Bhattacharjee, C., and Bhattacharya, P. K. *J. Membr. Sci.* **82**, 1 (1993).

[19] Richard, G. R., and Duong, D. D. (1994). *Applied Mathematics and Modeling for Chemical Engineers*, John Wiley & Sons Inc.

[20] Bowen, R. W., and Jenner, F. *Adv. Coll. Inter. Sci.* **56**, 141 (1995).

[21] Vilker, V. L., Colton, C. K., and Smith, K. A. *J. Coll. Inter. Sci.* **79**, 548 (1981).

[22] Gill, W. N., Wiley, D. E., Fell, C. J. D., Fane, A. G. *AIChE J.* **34**, 1563 (1988).

[23] Philles, G. D., Benedek, G. B., and Mazer, N. A. *J. Chem. Phys.* **65**, 1883 (1976).

[24] Jaan, K. (2005). *Numerical Methods in Engineering with MATLAB*, Cambridge University Press, UK.

[25] Carme, G., and Robert, H. D. *J. Membr. Sci.* **119**, 269 (1996).

[26] Bhattacharjee, C., and Datta, S. *Sep. Puri. Tech.* **24**, 13 (2001).